Proton Pump Inhibitors Induce Apoptosis of Human B-Cell Tumors through a Caspase-Independent Mechanism Involving Reactive Oxygen Species

Angelo De Milito,[1] Elisabetta Iessi,[1] Mariantonia Logozzi,[1] Francesco Lozupone,[1] Massimo Spada,[2] Maria Lucia Marino,[1] Cristina Federici,[1] Maurizio Perdicchio,[1] Paola Matarrese,[1] Luana Lugini,[1] Anna Nilsson,[3] and Stefano Fais[1]

[1]Department of Drug Research and Evaluation, Pharmacogenetic, Drug Resistance, and Experimental Therapeutic Section; [2]Department of Cell Biology, Istituto Superiore di Sanità, Rome, Italy; and [3]Microbiology and Tumorbiology Center, Karolinska Institute, Stockholm, Sweden

Abstract

Proton pumps like the vacuolar-type H^+ ATPase (V-ATPase) are involved in the control of cellular pH in normal and tumor cells. Treatment with proton pump inhibitors (PPI) induces sensitization of cancer cells to chemotherapeutics via modifications of cellular pH gradients. It is also known that low pH is the most suitable condition for a full PPI activation. Here, we tested whether PPI treatment in unbuffered culture conditions could affect survival and proliferation of human B-cell tumors. First, we showed that PPI treatment increased the sensitivity to vinblastine of a pre-B acute lymphoblastic leukemia (ALL) cell line. PPI, *per se*, induced a dose-dependent inhibition of proliferation of tumor B cells, which was associated with a dose- and time-dependent apoptotic-like cytotoxicity in B-cell lines and leukemic cells from patients with pre-B ALL. The effect of PPI was mediated by a very early production of reactive oxygen species (ROS), that preceded alkalinization of lysosomal pH, lysosomal membrane permeabilization, and cytosol acidification, suggesting an early destabilization of the acidic vesicular compartment. Lysosomal alterations were followed by mitochondrial membrane depolarization, release of cytochrome *c*, chromatin condensation, and caspase activation. However, inhibition of caspase activity did not affect PPI-induced cell death, whereas specific inhibition of ROS by an antioxidant (*N*-acetylcysteine) significantly delayed cell death and protected both lysosomal and mitochondrial membranes. The proapoptotic activity of PPI was consistent with a clear inhibition of tumor growth following PPI treatment of B-cell lymphoma in severe combined immunodeficient mice. This study further supports the importance of acidity and pH gradients in tumor cell homeostasis and suggests new therapeutic approaches for human B-cell tumors based on PPI. [Cancer Res 2007;67(11):5408–17]

Introduction

The hypoxic conditions and consequent acidity of tumor microenvironment play a key role contributing to tumor progression, chemoresistance, and metastatic behaviour (1, 2). Cancers face acidity with an up-regulated proton extrusion activity that allows tumor cells to survive in this unfavorable condition (3–5). Moreover, increasing evidence suggests that acidic vesicles play a role in tumor homeostasis and growth. An indirect evidence is provided by the fact that metastatic cells express more lysosomal proteins on the cell surface, suggesting that an aberrant compartmentalization of lysosomal-like activity operates in malignant tumor cells (6, 7).

A key mechanism controlling cellular pH is mediated by vacuolar-type H^+ ATPases (V-ATPase; ref. 8), ATP-dependent proton transporters that are normally expressed in intracellular compartments like lysosomes, endosomes, and secretory vesicles and on plasma membrane as well (8, 9). The up-regulated V-ATPase activity (10–12) and increased membrane V-ATPase expression detected in some human tumors are associated with chemoresistance and metastatic behavior of cancer cells (13). Classic V-ATPase inhibitors (e.g., bafilomycins) induce cell death in tumor cell lines (14), but these compounds are highly toxic and not suitable for clinical use in humans. Recently, it has been shown that *in vivo* inhibition of V-ATPase activity by RNA interference significantly delays human cancer growth by decreased proton extrusion (15), suggesting that pH regulation may have a key role in tumor homeostasis.

Human B-cell tumors, including acute lymphatic leukemia (ALL) and lymphomas, are currently treated with poly-chemotherapies resulting in good response rates (16, 17). However, a relevant proportion of patients is not cured from the disease because of chemoresistance and/or relapses. Moreover, recent therapy improvements have been often achieved by dose intensification, paying the price of severe toxicity and secondary malignancies (17, 18). Thus, preclinical studies on novel therapeutic approaches are needed.

Proton pump inhibitors (PPI), like omeprazole and esomeprazole, are the standard of treatment for acid-related diseases (19). They act as potent inhibitors of the gastric acid pump and have been used for short- or long-term treatments also with very high doses (150 mg/d) without major side effects (19, 20). Besides targeting the gastric acid pump, PPI inhibit the V-ATPase activity (21–23). We reported that PPI sensitize chemoresistant human tumors to cytotoxic drugs (24), suggesting that proton pump activity may affect cancer cells homeostasis and particularly acidic vesicles trafficking (5, 24). Moreover, it is known that PPI need an acidic environment to be fully activated, in turn suggesting a specific delivery for acidic environment, such as tumors (5, 25). Thus, we hypothesized that inhibition of proton pumps activity by PPI might deprive tumor cells of an important homeostatic mechanism, in turn leading to cell death.

Note: Supplementary data for this article are available at Cancer Research Online (http://cancerres.aacrjournals.org/).

Requests for reprints: Angelo De Milito, Department of Drug Research and Evaluation, Pharmacogenetic, Drug Resistance, and Experimental Therapeutic Section, Istituto Superiore di Sanità, Viale R. Elena 299, 00161, Rome, Italy. Phone: 39-06-49902153; Fax: 39-06-49903691; E-mail: Angelo.demilito@iss.it.

doi:10.1158/0008-5472.CAN-06-4095

Materials and Methods

Reagents and chemicals. Omeprazole and esomeprazole sodium salts were kindly provided by Astra-Zeneca and resuspended in saline (NaCl, 0.9%) at a concentration of 1 mg/mL immediately before use, following the instructions of the manufacturer. Vinblastine sulfate (Eli Lilly) was resuspended in saline at a concentration of 10 mg/mL and used within 1 week. Bafilomycin A1 and nigericin (Sigma) were respectively resuspended in DMSO and ethanol and used at the indicated concentrations. The pan-caspase inhibitor z-VAD-fmk (Calbiochem) was used at 50 to 200 μmol/L, and recombinant Fas ligand (R&D Systems) was used at 200 ng/mL. N-acetylcysteine (NAC), hydrohetidine, and acridine orange were from Molecular Probes.

Cell culture and clinical samples. The cell lines Daudi and Raji (human B-cell lymphomas), Nalm-6 (pre-B ALL), and Jurkat (T-cell leukemia) were kept in culture with RPMI 1640 (Cambrex) supplemented with antibiotics (Sigma) and 10% FCS (Cambrex). Unbuffered culture medium was prepared without sodium carbonate. Bone marrow aspirations were obtained from five children attending the Astrid Lindgren Hospital (Stockholm, Sweden) at diagnosis of pre-B ALL (Supplementary Table S1). ALL bone marrow cells were purified by Ficoll-Hypaque (Pharmacia) gradient separation and frozen in liquid nitrogen until analysis. For cell death experiments, the viability of cryopreserved bone marrow cells was measured immediately after thawing by trypan blue exclusion, and only cells with viability >90% were used in the study. Monocyte-derived macrophages (MDM) were obtained from healthy donors ($n = 3$) through magnetic cell sorting with anti-CD14 beads (Miltenyi Biotec) following manufacturer's instructions. The purified cells were seeded in 24-well plates (0.5×10^6 per well) for 5 days and then used for analysis of PPI toxicity in unbuffered culture medium. The ethical committees at the Karolinska Hospital and Istituto Superiore di Sanità approved the study, and samples were collected after informed consent from the parents of ALL children and from healthy donors in accordance with the Declaration of Helsinki.

Proliferation assay. The B-cell lines were plated in 96-well plates at a concentration of 10,000 per milliliter (200 μL per well) in buffered and unbuffered medium. The next day, omeprazole (or esomeprazole) was added to the wells at increasing concentrations (0, 17, 35, 70, and 140 μmol/L). The cells were kept in culture for 2 days, and thymidine incorporation was measured by adding 1 μCi ^{3}H-labeled thymidine per well (Pierce Biotechnology) to the cultures for the last 18 h. All experiments were run in triplicate wells and repeated at least twice.

Cell death and apoptosis determination. The effects of PPI pretreatment on vinblastine cytotoxicity were evaluated on Nalm-6 cells. Cells were cultured overnight in unbuffered medium, and PPI were added 8 or 24 h before the addition of different concentrations of vinblastine. Three days later, the cells were stained with 0.05% trypan blue for 10 min at room temperature and analyzed by fluorescence-activated cell sorting (FACS) in the FL3 channel to determine the percentage of dead cells.

For experiments on the direct cytotoxic effects of PPI, cell lines were cultured in unbuffered medium at 0.25×10^6 per milliliter in 24- to 48-well plates in duplicate wells and incubated overnight. The next day, PPI were added, and after 2 days, the cells were collected and analyzed. Cell viability was evaluated by trypan blue exclusion dye as above. Determination of apoptosis was done by staining the cells with Annexin V-FITC and propidium iodide (PI) following manufacturer's instructions (BD PharMingen), and apoptotic cells were defined as Annexin V–positive cells. Cells were sorted on a Becton Dickinson FACScan machine, and at least 10,000 cells per sample were analyzed using CellQuest software (Becton Dickinson Systems).

The effects of omeprazole treatment on leukemic blasts from patients with pre-B ALL were evaluated on bone marrow–purified mononuclear cells. The cells were cultured in unbuffered medium at 1×10^6 per milliliter in 96-well plates in duplicate wells and incubated overnight. Omeprazole (0–200 μmol/L) was added the next day, and apoptosis was measured 2 days after treatment. The analysis was done on the gate of bone marrow cells previously shown to be represented by >90% CD19$^+$ leukemic cells (26).

Lysosomal stability assessment. LysoTracker probes (Molecular Probes) and acridine orange accumulate in lysosomes and are used for the staining and semiquantitative evaluation of acidic intracellular organelles by fluorescence microscopy and FACS (27). The probes were used according to manufacturer's indications to measure the effects of PPI treatment on acidic vesicle pH, presence, and distribution. For the evaluation of lysosomal permeability, cells were incubated with LysoTracker Green DND-26 (1 μmol/L, 30 min at 37°C) or acridine orange (5 μmol/L, 10 min at 37°C) and analyzed by FACS. The experiments were repeated at least thrice in duplicate wells, and untreated and unstained cells were used to set the background fluorescence.

Evaluation of lysosomal acidity. LysoSensor Green DND-189 accumulates in lysosomes and acidic organelles (28). The probe exhibits a pH-dependent increase in fluorescence intensity on acidification and was used to monitor changes in the pH of acidic vesicles. Human B-cell lines (0.5×10^5 cells) were collected from untreated cultures and after PPI treatment at different time points and washed twice in PBS. The cells were incubated for 1 min at 37°C with 500 μL pre-warmed PBS containing 1 μmol/L LysoSensor probe, then immediately transferred on ice and analyzed by flow cytometry collecting FL1 fluorescence within 2 min. Statistical analysis was done by the parametric Kolmogorov-Smirnov test on a population of at least 20,000 cells.

Cytochrome *c* quantification. The amount of cytosolic cytochrome *c* in Nalm-6 cells was quantified by using a commercially available ELISA kit following the instructions from the manufacturer (R&D Systems).

Caspase activation. The activation of caspase-3, caspase-8, and caspase-9 was measured by using the caspase-specific CaspGLOW FITC kit with slight modifications (MBL International). Briefly, 0.1×10^6 cells untreated or treated with omeprazole or esomeprazole were collected and washed once in PBS. The cells were then resuspended into 100 μL Wash Buffer containing 0.33 μL of the caspase-specific FITC-conjugated peptide and incubated at 37°C for 60 min. After one wash in wash buffer, the cells were analyzed by FACS.

Detection of reactive oxygen species. Analysis of reactive oxygen species (ROS) production was evaluated on 0.25×10^6 cells at different time points after PPI treatments. The cells were incubated with 10 μmol/L dihydroethidium for 10 min at 37°C and analyzed by FACS. Hydrohetidine is a membrane-permeable dye that is oxidized in the presence of ROS and binds to double-stranded DNA, thus giving a deep red fluorescence detected in the FL3 channel.

Evaluation of cytosolic pH. The effects of PPI on cytosolic pH was evaluated by flow cytometry using the pH-sensitive fluorescent probe BCECF-AM (Molecular Probes) as previously described (29). About 10×10^6 cells were incubated at 37°C for 30 min in 1 mL RPMI containing 20 μmol/L BCECF-AM. The cells were then washed in HBSS, placed on ice, and analyzed with a FACSCalibur equipped with a 488-nm argon laser collecting the emission of BCECF-AM in the FL1 and FL2 channels. The relative cytosolic pH of individual cells was displayed in the two-dimensional dot-plot showing their fluorescence intensity at 520 nm (FL1, base) and 640 nm (FL2, acid) as described in details previously (29, 30). The BCECF-AM loaded cells were incubated with different potassium phosphate buffers in a range of pH from 5.5 to 7.5 in the presence of nigericin (10 μmol/L) to obtain a calibration curve (29).

Analysis of mitochondrial membrane potential. The status of the mitochondrial membrane potential ($\Delta\Psi$) was evaluated by using the JC-1 probe (Molecular Probes). Cells were stained with 10 μmol/L JC-1 for 15 min at 37°C and then immediately transferred on ice and analyzed by FACS (31).

Western blot analysis. Cytosolic and mitochondria-enriched cellular fractions were isolated from 5×10^6 Nalm-6 cells treated or not with omeprazole (200 μmol/L) by using the Q-Proteome Cell Compartment kit (Qiagen). SDS-PAGE was done on acrylamide gels (12%) loading 20 μg of subcellular fraction per lane. After electrophoresis, the proteins resolved on the gel were transferred to nitrocellulose membrane and blocked overnight with 5% dry milk in PBS. Apoptosis-inducting factor (AIF) and cytochrome *c* were detected with a rabbit anti-AIF (1:1,000; BD PharMingen) and mouse anti-cytochrome *c* (1:1,000; BD PharMingen) followed by specific horseradish peroxidase–conjugated secondary antibodies. Antibody staining was visualized by enhanced chemiluminescence (Pierce). To assess the presence on the filter of a comparable amount of proteins, the blots were stripped to detect actin.

Tumor growth in severe combined immunodeficient mice. Four- to 5-week-old female CB.17 severe combined immunodeficient (SCID/SCID) mice (Harlan) were used and kept under specific pathogen-free conditions

according to our institutional guidelines. Each mouse was injected s.c. in the right flank with 4×10^6 Raji cells resuspended in 0.2 mL RPMI 1640. When tumors appeared (~20 days after injection), omeprazole resuspended in saline was orally administered at a dose of 2.5 mg/kg for six times with 1-day interval, whereas mice in the control group were treated with saline. Tumor weight was measured every 6 days with calipers and estimated with the following formula: tumor weight (grams) = length (mm) $\times$ width^2 (mm) / 2. The experiment was interrupted when tumor mass exceeded 10% of total body weight, and all experimental procedures were carried out according to the United Kingdom Co-ordinating Committee on Cancer Research guidelines.

Statistical analysis. Differences between groups or treatments were analyzed by Student's *t* test, and the statistically significant differences were defined only when $P < 0.05$. Means and SDs were calculated from at least three independent experiments.

Results

PPI pretreatment increases pre-B ALL cell line sensitivity to vinblastine. We previously reported that 24 h of omeprazole pretreatment induced sensitivity of various human tumor cell lines to chemotherapeutics (24). Here, we tested whether pretreatment

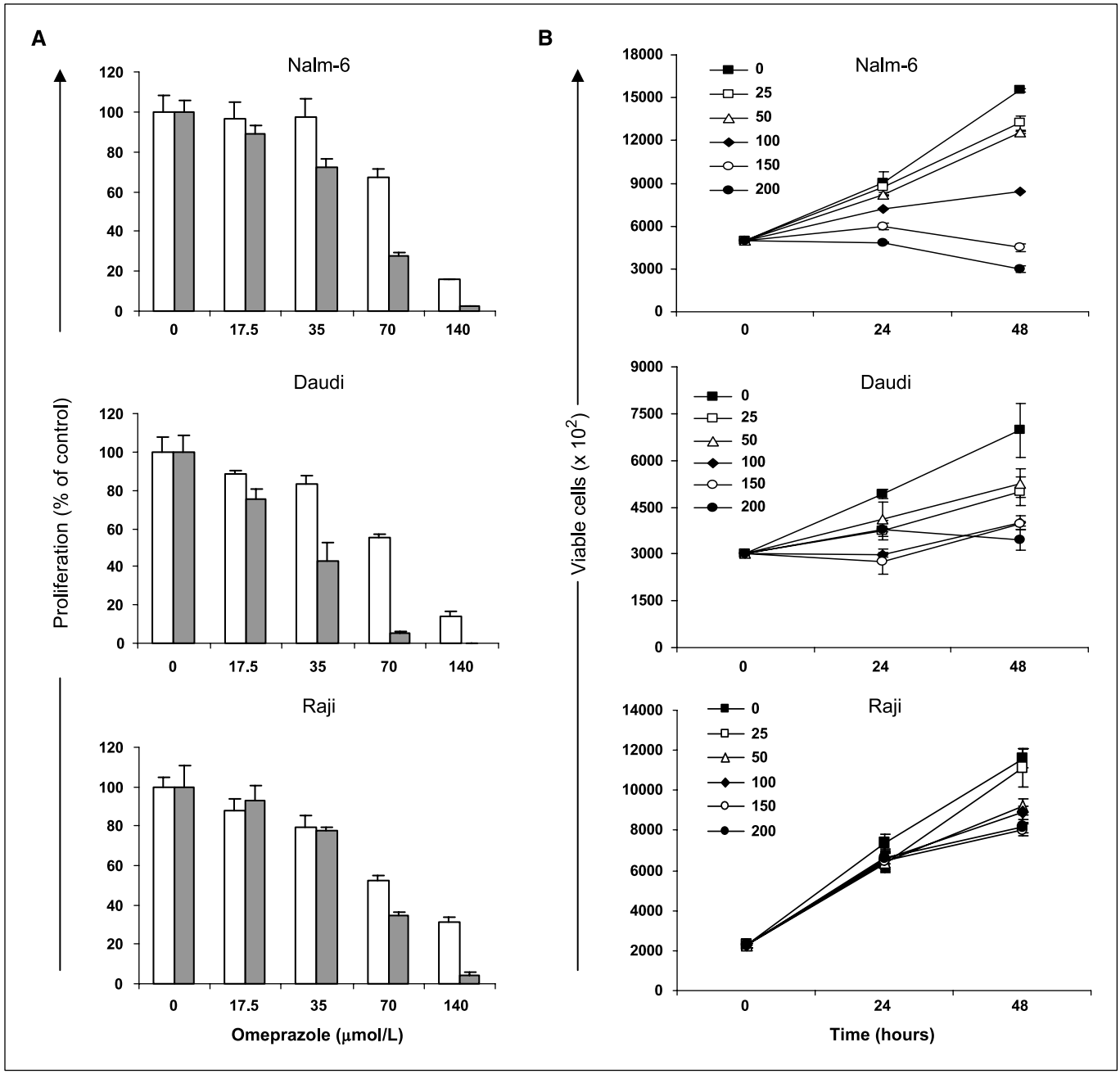

Figure 1. PPI affect proliferation and viability of human B-cell lines. *A,* Daudi, Raji, and Nalm-6 cells were cultured in buffered (*white columns*) or unbuffered (*gray columns*) medium overnight. Different doses of omeprazole were added, and thymidine incorporation was evaluated after 2 d. *Columns,* mean proliferation rate as percentage of untreated cells of two independent experiments; *bars,* SD. *B,* Daudi, Raji, and Nalm-6 cells were cultured in unbuffered culture medium overnight. Omeprazole was added at increasing concentrations, and cell viability was measured by trypan blue staining at indicated times. *Points,* means of two independent experiments run in triplicate; *bars,* SD.

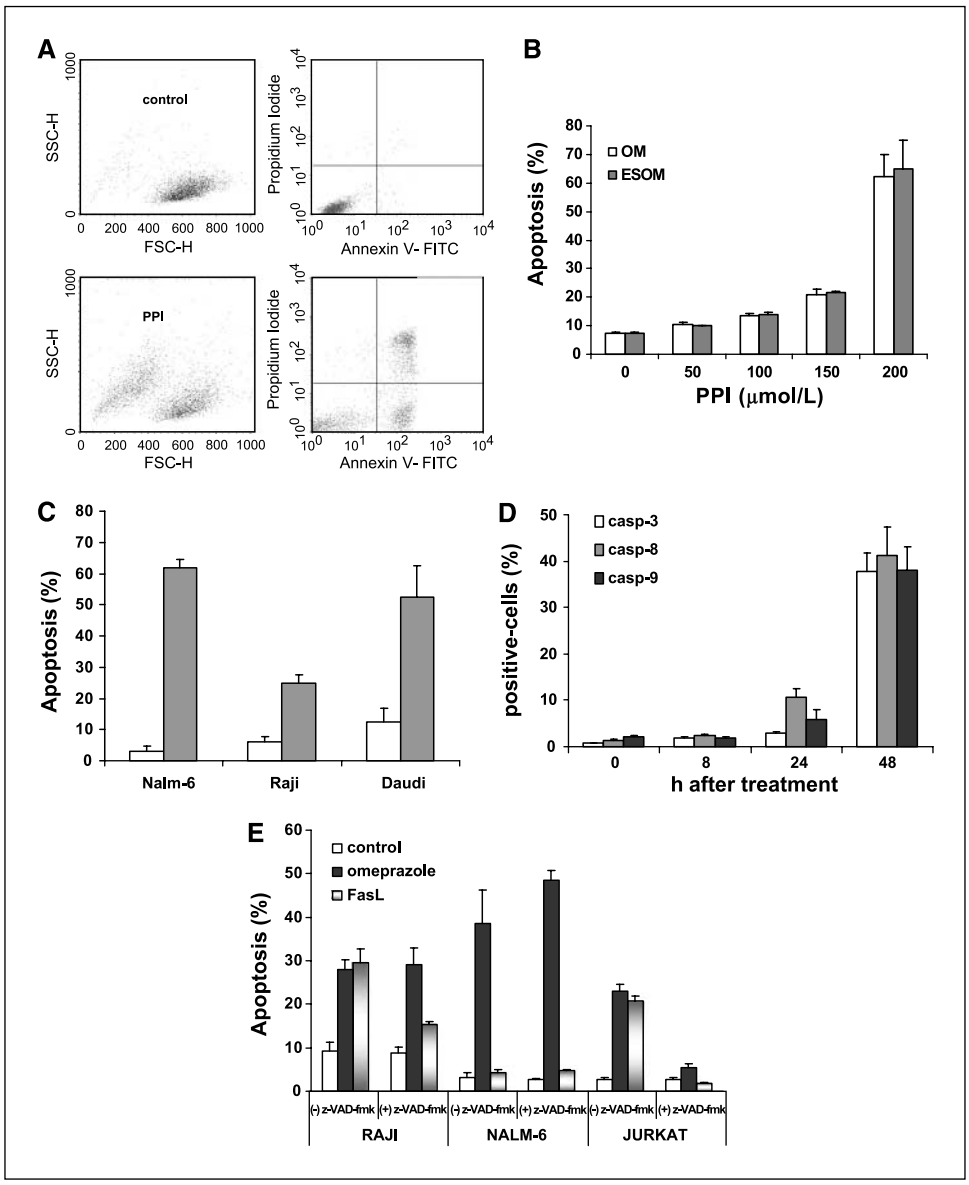

Figure 2. PPI induce caspase-independent apoptosis in human B-cell lines. *A,* representative FACS analysis of the cytotoxic effects of 48 h of omeprazole treatment (200 μmol/L) in Nalm-6 cells cultured in unbuffered conditions. Morphologic variables (*left*) and dot plot for Annexin V and PI staining (*right*) for untreated and treated cells. *B,* apoptotic effects of omeprazole (*OM*) and esomeprazole (*ESOM*) on Nalm-6 treated for 2 d with increasing doses of the drugs. *C,* the level of PPI-induced apoptosis on the three B-cell tumor lines. Apoptosis was defined as the percentage of Annexin V–positive cells. *D,* the presence of activated caspase-3 (*casp-3*), caspase-8 (*casp-8*), and caspase-9 (*casp-9*) was detected in Nalm-6 cells by FACS. *E,* effects of pan-caspase inhibitor on apoptosis induced by PPI (200 μmol/L) and Fas ligand (*FasL*; 200 ng/mL) was evaluated on Raji, Nalm-6, and Jurkat cells after 48 h. *Columns,* means of three independent experiments run in duplicate; *bars,* SD.

with omeprazole and esomeprazole was able to increase the sensitivity of a B-cell leukemia (Nalm-6), already sensitive to cytotoxic effect of vinblastine, commonly used in the treatment of ALL (32). Because PPI need an acidic pH to be protonated and activated (33), we evaluated the effect of omeprazole and esomeprazole in unbuffered culture conditions to allow cells spontaneously acidify the culture medium. Indeed, whereas the pH of a buffered medium decreased from 7.7 ± 0.1 to 7.4 ± 0.2 after 24 h in culture (0.3 pH units), the pH of unbuffered medium changed from 7.2 ± 0.1 to 6.5 ± 0.2 (0.7 pH units), thus providing the acidic conditions for a better activation of the PPI. Cell viability and growth were not affected in these conditions (data not shown). Nalm-6 cells were pretreated with PPI (13 μmol/L) for 24 h and then treated with increasing doses of vinblastine, and after 3 days, cell viability was evaluated by FACS analysis of cells stained with trypan blue. At this dose, omeprazole and esomeprazole pretreatment was not toxic to the cells per se but significantly increased the sensitivity of Nalm-6 cells to the cytotoxicity induced by vinblastine (Supplementary Fig. S1), significantly reducing the IC_{50} for vinblastine ($P < 0.01$). We observed that this effect was detectable also after 8 h of pretreatment with PPI (data not shown) and was comparable with the ability of PPI to increase vinblastine sensitivity of CEM cells previously reported by us (24).

PPI inhibit proliferation and affect viability of human B-cell lines. We reported that low-dose PPI induces alterations of pH gradients of tumor cells without affecting cell viability (5, 24). Because proper regulation of cellular pH gradients is crucial for cell homeostasis (34), we evaluated whether PPI treatment affected viability and proliferation of human B-cell tumors *in vitro*. Because we observed that a more acidic pH of unbuffered medium may better activate PPI, we measured the proliferation of human B-cell lines in buffered and unbuffered culture medium in presence of PPI. Omeprazole induced a dose-dependent inhibition of cell proliferation in both leukemia and lymphoma B cells (Fig. 1*A*), with similar results observed for esomeprazole (data not shown). As expected, the concentration of omeprazole inducing a 50%

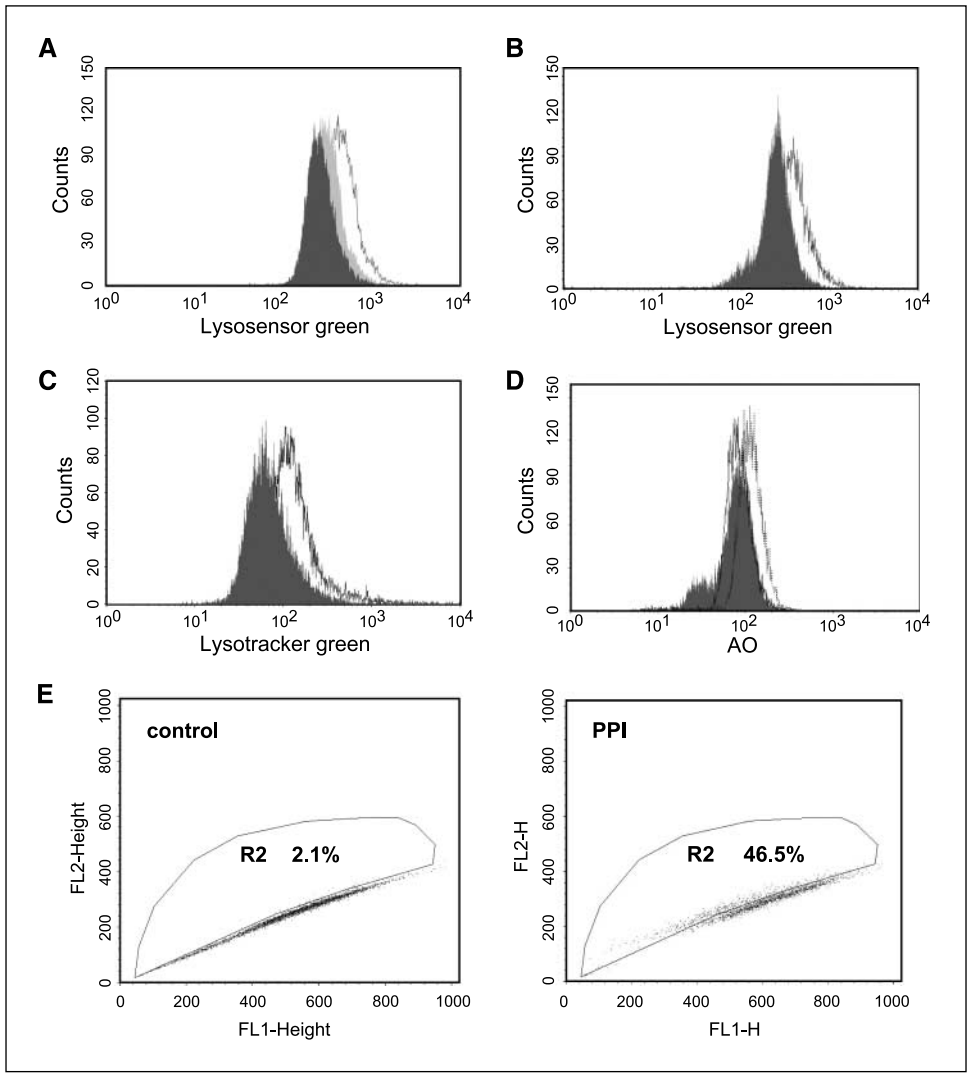

Figure 3. PPI induce early destabilization of lysosomal-like vesicles and cellular pH gradients. Nalm-6 cells were cultured in unbuffered medium without PPI (*black lines*) and in the presence of PPI (*filled areas*). The variation of intravesicular pH and the status of lysosomal permeability were measured by FACS analysis of cells stained with LysoSensor Green DND-189 and Lysotracker or acridine orange as described in Materials and Methods. *A,* effects of two concentrations of omeprazole (25 and 200 μmol/L, respectively, *light* and *dark gray fill*) on lysosomal pH was analyzed 24 h after treatment. *B,* cells were treated with omeprazole (200 μmol/L), and the lysosomal pH was evaluated after 8 h. *C,* LysoTracker Green DND-26 staining of Nalm-6 cells treated with 200 μmol/L omeprazole for 2 d. Untreated cells (*empty histograms*) and treated cells (*gray histograms*). *D,* Nalm-6 cells were stained with acridine orange (*AO*) before (*dotted line*), 8 h (*black line*), and 24 h (*dark gray fill*) after addition of omeprazole (200 μmol/L). *E,* change in cytosolic pH induced by omeprazole (200 μmol/L) was evaluated in Nalm-6 cells treated for 48 h and loaded with the pH-sensitive fluorescent probe BCECF-AM. The population in the region R2 contains cells with a more acidic intracellular pH as indicated by a lower FL1/FL2 ratio. All experiments were run twice, and similar results were obtained for Raji and Daudi cells.

reduction of cell proliferation was lower in unbuffered compared with buffered culture conditions (57.3 ± 4.5 versus 86.2 ± 6.2 μmol/L, $P = 0.01$).

To test whether the antiproliferative effect was dependent on PPI-induced cytotoxicity, PPI were added to the cultures 1 day after plating the cells, and viability was measured 24 and 48 h after by FACS analysis of trypan blue–stained cells. We found that omeprazole and esomeprazole (data not shown) induced a time- and dose-dependent decrease in cell viability (Fig. 1*B*), with a slight difference in sensitivity among the three cell lines, reflecting the data of the proliferation experiments.

PPI induce a caspase-independent, apoptotic-like cell death in human B-cell lines. To investigate the mechanisms leading to loss of cell viability, we tested membrane integrity and the presence of phosphatidylserine residues on the outer membrane as markers of apoptotic cells. PPI-induced cell death measured after 48 h was characterized by the presence of Annexin V–positive cells (Fig. 2*A*), which was detectable 24 h after treatment with the appearance of Annexin V^+/PI^- cells (data not shown), indicating the activation of an apoptotic pathway. In line with this observation, nuclear fragmentation was observed 48 h after treatment (data not shown). The PPI-induced apoptosis was dose dependent (Fig. 2*B*) and observed in all the B-cell lines tested (Fig. 2*C*).

To evaluate the contribution of active caspases in PPI-induced apoptosis, we evaluated the percentage of cells carrying activated caspase-3, caspase-8, and caspase-9 and found that the presence of activated caspases in Nalm-6 cells was detected in about 50% of cells 48 h after treatment (Fig. 2*D*), with similar results obtained on Raji and Daudi cells (data not shown). However, caspase inhibition through the pan-caspase inhibitor z-VAD-fmk, while decreasing Fas-mediated apoptosis in Raji cells, had no effect on PPI-induced cytotoxicity of both Raji and Nalm-6 cells (Fig. 2*E*), suggesting that activated caspases are not instrumental for PPI-induced apoptosis in B-cell tumors. In line with this and previous observations (35), apoptosis induced by Bafilomycin A1 on B cells was also caspase independent (data not shown). As previously reported (36), PPI-induced apoptosis in Jurkat cells was caspase dependent (Fig. 3*E*), suggesting that a different pathway is responsible for the cytotoxicity of PPI in B-cell tumors.

PPI induce early lysosomal membrane permeabilization in human B-cell lines. Mechanisms controlling the pH of intracellular organelles seem to have a pivotal role in maintaining cell homeostasis and in regulating cell death (34). Low-dose PPI (2.5–13 μmol/L) affects pH gradients in solid tumor cell lines (24). Here, we analyzed the long-term effects of a wide range of PPI concentrations (0–200 μmol/L) on intracellular vesicles pH in

human B-cell lines. Lysosensor staining showed that PPI induced a dose-dependent alkalinization of intracellular acidic compartments (Fig. 3*A*), detectable already 8 h after treatment (Fig. 3*B*). Staining with acridine orange and LysoTracker Green showed that a decreased fluorescence intensity was also observed 8 h after treatment with PPI (Fig. 3*C* and *D*). Altogether, these findings clearly indicated that PPI induce early alterations in the lysosomal compartment consisting of lysosomal pH alkalinization and lysosomal membrane permeabilization (LMP).

Because cathepsins localize in lysosomes and may be used as markers of lysosomal membrane disruption (27), we analyzed a possible involvement of cathepsins in the PPI-induced apoptosis. We observed that lysosomal membrane rupture occurred very late in the process (48 h after PPI treatment) as shown by fluorescence analysis of cathepsin B and D intracellular localization (Supplementary Fig. S2). Consistent with these late events, inhibition of cathepsins B and D did not affect the PPI-mediated cytotoxicity.

Acidification of cytosolic pH occurs in PPI-induced cell death. It has been reported that the acidification of cytosolic pH precedes apoptosis of leukemia/lymphoma cells (37, 38). Because PPI may inhibit one of the crucial mechanism regulating cellular pH, we analyzed the changes in the cytosolic pH following PPI treatment in Nalm-6 cells up to 48 h. We found that after 24 h of PPI treatment, the cytosolic pH of PPI-treated cells was 7.12 $\pm$ 0.04, whereas the cytosolic pH of control cells was 7.21 $\pm$ 0.01. As reported in Fig. 3*E*, 48 h of PPI treatment induced the appearance of a population of cells with acidic cytosolic pH (6.21 $\pm$ 0.03 versus 7.30 $\pm$ 0.01). In the PPI-treated samples, the cells characterized by a decreased FL1/FL2 ratio (indicating an acidic cytosolic pH) were identified by forward and side light scatter as apoptotic cells (data not shown), suggesting that cytosolic acidification and cell shrinkage were associated.

Mitochondrial membrane depolarization occurs in PPI-induced cell death. The lysosomal-mitochondrial pathway mediates cell death induced by different stimuli, including lysosomotropic agents (27, 39, 40). Thus, we evaluated the effects of PPI treatment on mitochondrial membrane potential ($\Delta\Psi$). All B-cell lines were treated for 2 days with PPI (50–200 μmol/L), and changes in $\Delta\Psi$ were analyzed after 8, 24, and 48 h. The depolarization of $\Delta\Psi$ was detected only after 24 h of treatment (Fig. 4*A*), with the presence of a cell population with an intermediate $\Delta\Psi$ (*top right quadrant*), representing early apoptotic cells (31), and a proportion of cells with a collapsed $\Delta\Psi$ (*bottom right quadrant*), representing late apoptotic cells. Moreover, accurate FACS analysis done on the gate of live cells (according to morphologic variables) showed similar results. The effects of PPI on mitochondrial function was also shown by the release of cytochrome *c* from mitochondria to the cytosol 24 h after addition of PPI, as shown by ELISA and Western blot (Fig. 4*B* and *C*). The permeabilization of the mitochondrial membrane was further shown by the partial release of AIF from mitochondria and the accumulation of AIF in the cytosolic fraction after 48 h, suggesting the involvement of AIF in the execution of the apoptotic process.

PPI-mediated cell death occurs via ROS-dependent mechanisms. Because ROS generation plays an important role in caspase-independent apoptosis (27, 41), we investigated whether ROS generation was required for triggering the lysosomal-mitochondrial cell death pathway. First, we observed that PPI (also at suboptimal doses like 50 μmol/L) induced a very early production of ROS detectable in the whole cell population within 4 h after treatment (Fig. 5*A, top*), and preincubation of PPI-treated cultures with the ROS scavenger NAC (5 mmol/L) totally abolished the PPI-mediated production of ROS (Fig. 5*A, bottom*) and significantly inhibited the cytotoxicity of PPI (Fig. 5*B*). This process was accompanied by a stabilization of the lysosomal membrane assessed by acridine orange staining (Fig. 5*C*) and by a reduction in the population of cells with a collapsed $\Delta\Psi$ (Fig. 5*D*), thus suggesting an important role of ROS in PPI-induced apoptosis.

PPI are cytotoxic for leukemic cells from patients with pre-B ALL. Because PPI exhibited a clear cytotoxic effect on human B-cell tumors *in vitro*, we investigated whether such cytotoxicity

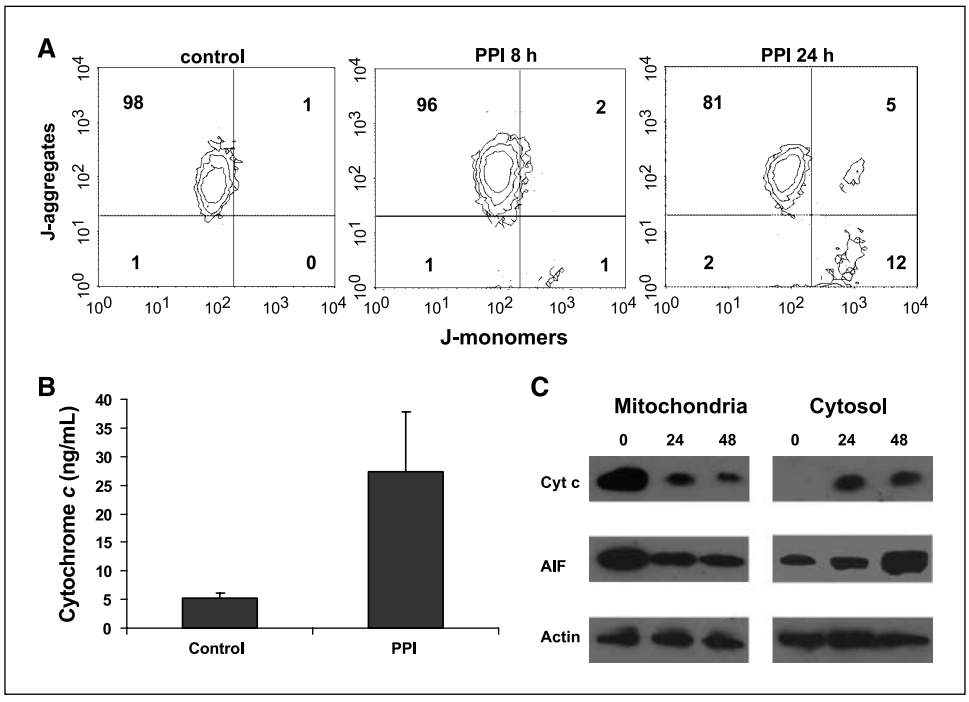

Figure 4. Analysis of mitochondrial membrane potential and permeability in PPI-treated B-cell tumors. *A,* representative FACS analysis of the mitochondrial membrane potential ($\Delta\Psi$) done by using JC-1 staining on Nalm-6 cells 8 and 24 h after treatment with PPI (200 μmol/L). The events in the bottom quadrants and/or in the top right quadrant represent cells with a depolarized $\Delta\Psi$. *B,* quantification of cytosolic cytochrome *c* measured by a commercial ELISA in Nalm-6 cells 24 h after treatment with PPI. *C,* Western blot analysis of the release of cytochrome *c* (*Cyt c*) and AIF from mitochondria to the cytosol in PPI-treated cells at different time points. All experiments were repeated at least twice.

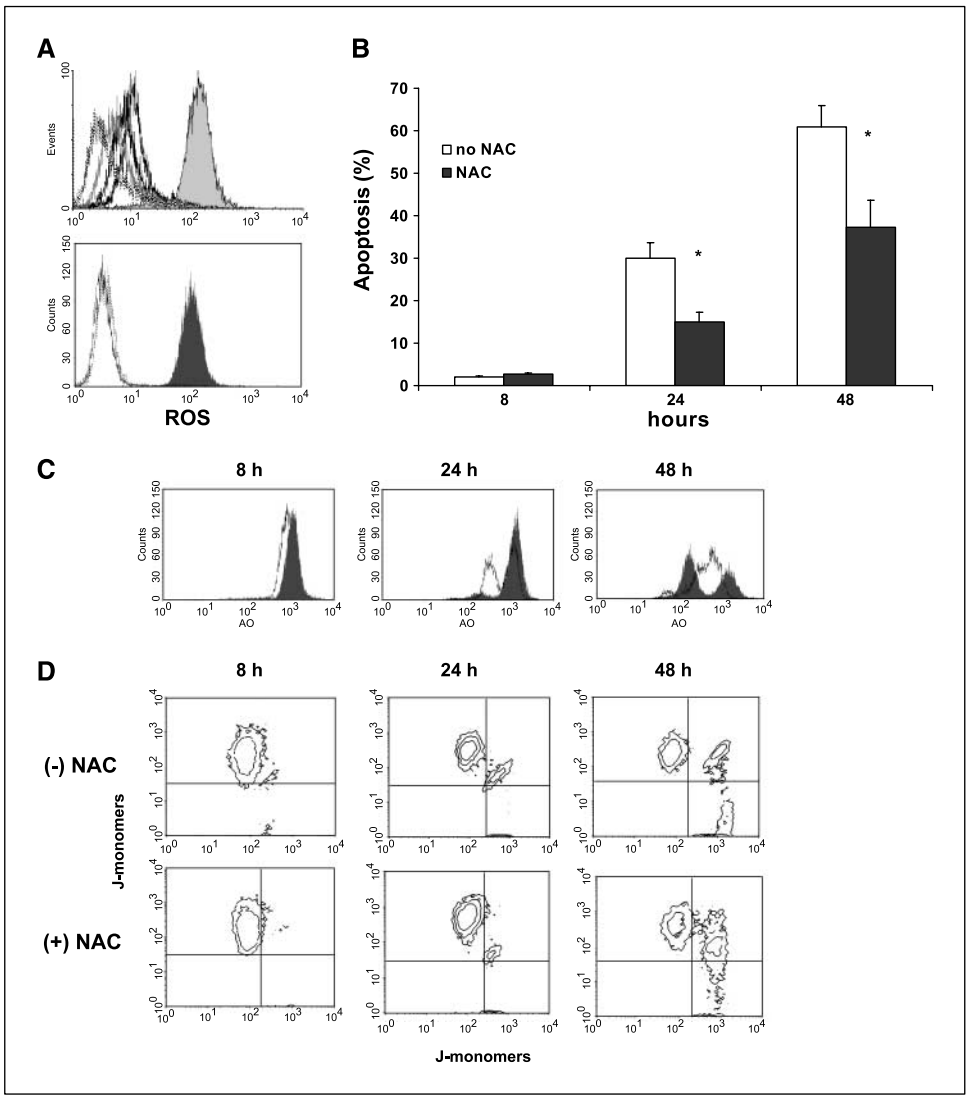

Figure 5. Involvement of ROS in PPI-mediated apoptosis of human B-cell tumors. *A, top,* Nalm-6 cells were treated with PPI, and the presence of ROS was measured by HE staining 0.5 h (*gray line*), 2 h (*black bold line*), 4 h (*black thin line*), and 8 h (*gray fill*) after treatment with respect to untreated cells (*dotted line*). *Bottom,* accumulation of ROS was measured on PPI-treated cells in the presence (*black line*) or absence (*gray fill*) of the ROS scavenger NAC (5 mmol/L). Unstained cells (*dotted line*). *B,* kinetics of PPI-induced apoptosis in Nalm-6 cells in the presence of NAC (5 mmol/L). *Columns,* means of four independent experiments run in duplicate; *bars,* SD. *C,* analysis of lysosomal membrane permeabilization detected as acridine orange fluorescence in PPI-treated Nalm-6 cells with (*gray fill*) or without (*black line*) NAC (5 mmol/L) at different time points. *D,* analysis of $\Delta\Psi$ by JC-1 staining in PPI-treated Nalm-6 cells with or without NAC (5 mmol/L) at different time points.

could also be observed *ex vivo* in bone marrow–derived leukemic cells isolated from pre-B ALL patients. Bone marrow cells were cultured in unbuffered medium in the presence of increasing concentrations of omeprazole, and apoptosis was measured after 2 days. We found that omeprazole induced a clear and dose-dependent cytotoxicity in all samples tested (Fig. 6*A*). Omeprazole concentrations of 100 and 200 μmol/L induced cell death in the ALL cells ranging between 28.8 ± 5.0% and 62.6 ± 9.6%, with a significant increase compared with baseline cell death of untreated controls (11.6 ± 1.9%, $P < 0.001$). Conversely, PPI had no toxic effect on MDM isolated from healthy subjects (Fig. 6*B*).

***In vivo* antitumoral effects of PPI treatment.** The antitumoral activity of PPI was evaluated *in vivo* in the SCID mouse tumor growth model. Because the doses of PPI used *in vitro* exceed the serum concentrations of PPI thus far reported in human studies, we decided to use a dose of omeprazole comparable with the doses used in *in vivo* studies (2.5 mg/kg; ref. 42). Control mice ($n = 7$) received saline, whereas treated mice ($n = 7$) received six doses of omeprazole, with 1-day interval and tumor growth was estimated during the follow-up. The growth of Raji tumors in mice treated with omeprazole was significantly reduced compared with control animals (Fig. 6*C*), and the size of PPI-treated tumors was significantly smaller than control tumors at follow-up ($P = 0.01$), indicating that PPI treatment may exert an antineoplastic activity *in vivo*.

Discussion

During the last decade, it has become evident that tumors hijack basic homeostatic cellular functions to progress towards malignancy. Such functions are involved in the control of cell proliferation, invasion capacity, and resistance to antitumoral treatments. An important function involved in malignant progression is the pH regulation, whose activity is abnormal in tumors. Such selective advantage is conferred to tumor cells by the capacity of surviving in hypoxic-acidic environment, mediated by the up-regulated lysosomal trafficking and proton extrusion activity (3–5, 43). In fact, whereas the extracellular pH of normal tissues is neutral, the interstitial pH of tumors is acidic, and because of this feature, tumor cells are characterized by two pH gradients: that between the cytosol and the extracellular matrix and the one between the cytosol and the lumen of intracellular vesicles (5). To avoid intracellular acidification

under such conditions, tumor cells have an increased activity of pH regulators, including the V-ATPase (44). In agreement with the effects of PPI on the endo-lysosomal compartment, we previously reported that decreasing the pH gradients in tumor cells through PPI may revert chemoresistance and increase chemosensitivity of different human tumor cells, including a T-cell leukemia line (24, 45).

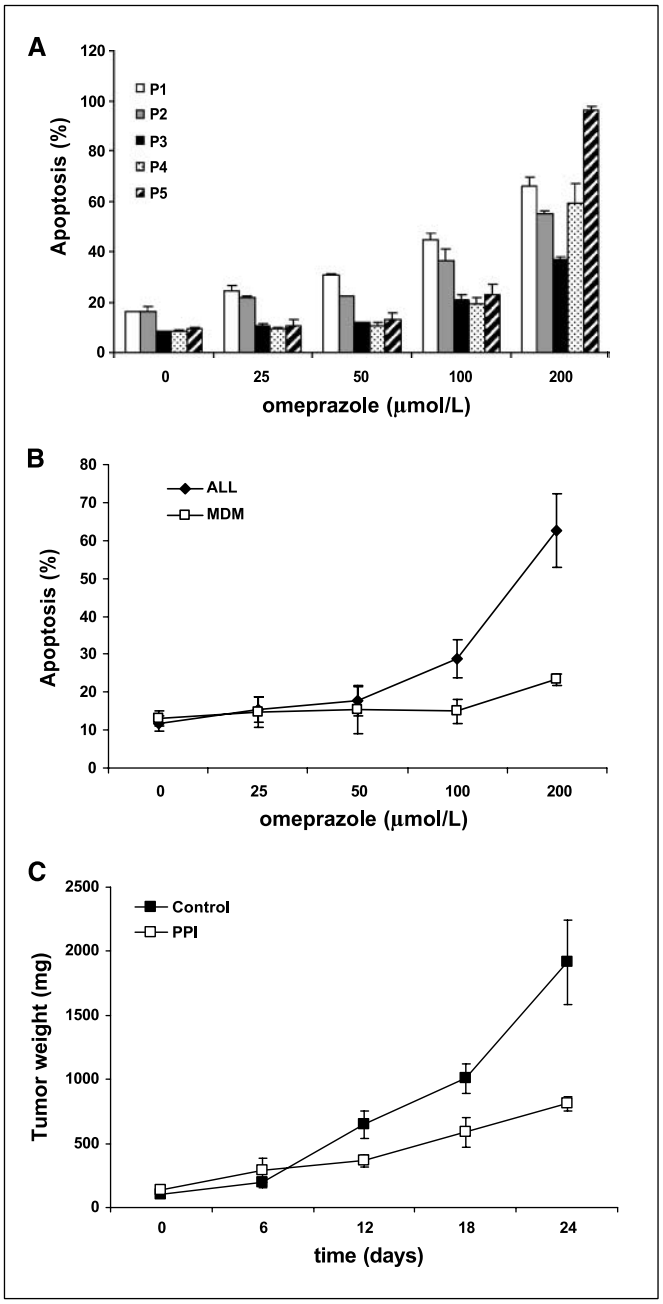

Figure 6. PPI induce apoptosis of B-cell tumors *ex vivo* and *in vivo. A,* leukemic cells purified from bone marrow of five ALL patients were cultured in presence of increasing concentrations of omeprazole, and apoptosis was evaluated after 2 d. Table with the clinical characteristics of the patients is shown in Supplementary Table S1. Age at diagnosis is expressed in years. WBC count, 10^6 cells per milliliter. *B,* cytotoxicity of omeprazole on ALL cells ($n = 5$) and human MDM cells from three healthy donors after 2 d of treatment. *Points,* mean; *bars,* SD. *C, in vivo* effects of PPI on tumor growth in the human tumor/SCID mouse model. Raji cells (4×10^6) were engrafted s.c. into SCID mice, and at tumor appearance, animals were treated ($n = 7$) or not ($n = 7$) with six doses omeprazole (2.5 mg/kg) given by gavage. Tumor growth was followed up for 24 d and expressed as tumor weight (g). *Points,* mean; *bars,* SD.

In fact, we confirmed in this study that PPI pretreatment of the human pre-B ALL cell line Nalm-6 significantly increased the sensitivity to vinblastine, a commonly used chemotherapeutic agent in ALL. In addition, we found that also a short preincubation time (8 h) with PPI was sufficient to observe this effect.

It has been suggested that targeting mechanisms allowing tumors to survive in acidic/hypoxic conditions may represent a novel strategy to combat cancer (34). PPI could represent a class of drugs suitable to this purpose. In fact, being the V-ATPase one of their targets, PPI may revert the pH gradients of tumor cells. Moreover, PPI are commonly administered to millions of subjects affected by peptic diseases, with minimal side effects and few drug interactions (19, 20). Consistently, omeprazole did not inhibit functions of human macrophages and lymphocytes in long-term treated patients (46). We know that PPI are weak bases, and the active protonated form of the drug will necessarily accumulate into acidic compartments (33). In fact, in healthy subjects, PPI mostly target the stomach, being the most acidic site of the body. Therefore, it seemed conceivable that PPI may specifically get to the tumor site, being an additional acidic compartment in cancer patients. We reasoned that any effect of PPI on tumor cells *in vitro* would be potentiated by the degree of acidity of the surrounding microenvironment, as already shown for its antimicrobial activity (47, 48). Indeed, although the doses at which PPI induced cell death *in vitro* are higher than plasma concentrations reached in humans at standard dosage, we believe that PPI may achieve higher local concentrations at tumor site. This may be true also in the case of hematologic malignancies with massive blast proliferation in acidic/hypoxic environment like the bone marrow. In fact, PPI showed a dose-dependent effect on cell viability inducing an apoptotic-like cell death in both human B-cell lines and bone marrow–derived leukemic blasts of pre-B ALL patients, without any significant effect on human MDM. In addition, *in vivo* treatment with PPI of Raji tumors injected into SCID mice significantly delayed tumor growth. Our observation supports data reporting that inhibition of V-ATPase activity by small interfering RNA delay tumor growth *in vivo* (15), and that pharmacologic inhibitors of V-ATPase induce cell death in B-cell lymphoma (14). Consistent with the hypothesis that because of the acidic pH of tumors, PPI may find a specific delivery to tumors rather than normal tissues, the antineoplastic effect of PPI was always stronger in unbuffered rather than buffered culture conditions, as supported by measurements of extracellular pH in cells cultured in the buffered and unbuffered conditions. This suggests that leaving tumor cells spontaneously acidify their environment markedly increases PPI activation due to acidity.

The apoptotic-like process induced by PPI involved the activation of different caspases whose role is, however, not instrumental. In fact, the pan-caspase inhibitor z-VAD-fmk did not inhibit PPI-mediated apoptosis in B-cell tumors, whereas it was able to inhibit apoptosis of Jurkat cells, confirming a previous report (36) and suggesting that PPI may act on B-cell tumors by a different mechanism. It is known that LMP induced by quinolone antibiotics triggers caspase-independent cell death through mitochondrial membrane permeabilization (MMP; ref. 27). In addition, the synthetic retinoid CD437 and a polyamine oxidase inhibitor induce apoptosis of hematopoietic tumor cells through lysosomotropic effects in a caspase-independent manner despite the presence of activated caspases (39, 40). We found that B-cell lines treated with PPI were characterized by early lysosomal alterations, detected as increased intraluminal pH and reduced membrane stability within

8 h after treatment. This effect was amplified during the following days, when also a destabilization of lysosomal vesicles content was shown by analysis of lysosomal markers like cathepsins B and D and Lamp-1 (data not shown). However, inhibition analysis of cathepsins activity showed no protection against PPI-induced cell death in B-cell lines (data not shown), indicating that PPI may lead to the simultaneous activation of different cell death pathways, most likely triggered by the profound disruption of cellular pH gradients. Interestingly, we found that mitochondrial membrane depolarization and release of cytochrome *c* occurred before the activation of caspases and after LMP, suggesting that PPI-induced cell death may follow the lysosomal-mitochondrial pathway. In addition, PPI caused the mitochondrial release of the caspase-independent death effector AIF. The importance of lysosomes in the apoptotic process was also confirmed by the finding that PPI induced a very early accumulation of ROS, which was inhibited by the ROS scavenger NAC. In fact, ROS inhibition by NAC significantly delayed PPI-induced apoptosis and caused the stabilization of the lysosomal compartment, in turn resulting in protection of mitochondria as it occurs in similar apoptotic pathways (49). Therefore, intracellular ROS generation seems to be a primary event induced by PPI, likely causing mitochondrial membrane depolarization, cytosolic release of AIF (and/or other proteins) from the mitochondria, and then apoptosis (50).

The alteration of the pH gradient between cytosol and lysosomal vesicles was further amplified by the concomitant acidification of cytosolic pH following PPI treatment. Interestingly, reduction in intracellular pH after inhibition of the Na^+/H^+ exchanger, another regulator of cellular pH, has been reported to induce apoptosis of primary patients' leukemic cells (37). This suggests that PPI induce cell death in B-cell tumors by breaking down the fine regulation of pH gradients, a homeostatic mechanism crucial for survival of tumor cells. We observed that the Daudi and Nalm-6 cells showed a higher sensitivity to PPI cytotoxicity compared with Raji cells. Interestingly, Raji cells had a cytosolic pH of 7.35, which was lower than that of Daudi and Nalm-6 cells (pH 7.5; data not shown). The possibility that PPI effects are strictly dependent upon proton pumps and ROS-generating enzymes is currently under investigation in our laboratory.

This study indicates that PPI induce cell death of human B-cell tumors through severe alteration of pH gradients regulation, including ROS production, LMP, and MMP. Clearly, the *in vivo* effectiveness of PPI depends on the ability of tumor cells to acidify their environment, to allow first the drug to target the tumor and then to be activated *in situ*. Our study suggests that mechanisms involved in regulation of cellular pH may represent suitable targets for novel antitumor strategies and indicates the potential use of PPI as antineoplastic agents towards human B-cell tumors.

Acknowledgments

Received 11/6/2006; revised 2/20/2007; accepted 4/2/2007.

Grant support: The study was partially supported by a collaborative project between ISS and AstraZeneca. Angelo De Milito was supported by a post-doctoral fellowship from the Swedish Research Council.

The costs of publication of this article were defrayed in part by the payment of page charges. This article must therefore be hereby marked *advertisement* in accordance with 18 U.S.C. Section 1734 solely to indicate this fact.

References

1. Raghunand N, He X, van Sluis R, et al. Enhancement of chemotherapy by manipulation of tumour pH. Br J Cancer 1999;80:1005–11.
2. Gatenby RA, Gillies RJ. Why do cancers have high aerobic glycolysis? Nat Rev Cancer 2004;4:891–9.
3. Gatenby RA, Gawlinski ET. The glycolytic phenotype in carcinogenesis and tumor invasion: insights through mathematical models. Cancer Res 2003;63:3847–54.
4. Sennoune SR, Luo D, Martinez-Zaguilan R. Plasmalemmal vacuolar-type H^+-ATPase in cancer biology. Cell Biochem Biophys 2004;40:185–206.
5. De Milito A, Fais S. Tumor Acidity, Chemoresistance and proton pump inhibitors. Future Oncology 2005;1:779–86.
6. Saitoh O, Wang WC, Lotan R, Fukuda M. Differential glycosylation and cell surface expression of lysosomal membrane glycoproteins in sublines of a human colon cancer exhibiting distinct metastatic potentials. J Biol Chem 1992;267:5700–11.
7. Glunde K, Guggino SE, Solaiyappan M, Pathak AP, Ichikawa Y, Bhujwalla ZM. Extracellular acidification alters lysosomal trafficking in human breast cancer cells. Neoplasia 2003;5:533–45.
8. Nishi T, Forgac M. The vacuolar (H^+)-ATPases: nature's most versatile proton pumps. Nat Rev Mol Cell Biol 2002;3:94–103.
9. Vaananen HK, Karhukorpi EK, Sundquist K, et al. Evidence for the presence of a proton pump of the vacuolar H(+)-ATPase type in the ruffled borders of osteoclasts. J Cell Biol 1990;111:1305–11.
10. Marquardt D, Center MS. Involvement of vacuolar H(+)-adenosine triphosphatase activity in multidrug resistance in HL60 cells. J Natl Cancer Inst 1991;83:1098–102.
11. Martinez-Zaguilan R, Lynch RM, Martinez GM, Gillies RJ. Vacuolar-type H(+)-ATPases are functionally expressed in plasma membranes of human tumor cells. Am J Physiol 1993;265:C1015–29.
12. Murakami T, Shibuya I, Ise T, et al. Elevated expression of vacuolar proton pump genes and cellular PH in cisplatin resistance. Int J Cancer 2001;93:869–74.
13. Sennoune SR, Bakunts K, Martinez GM, et al. Vacuolar H^+-ATPase in human breast cancer cells with distinct metastatic potential: distribution and functional activity. Am J Physiol Cell Physiol 2004;286:C1443–52.
14. Nishihara T, Akifusa S, Koseki T, Kato S, Muro M, Hanada N. Specific inhibitors of vacuolar type H(+)-ATPases induce apoptotic cell death. Biochem Biophys Res Commun 1995;212:255–62.
15. Lu X, Qin W, Li J, et al. The growth and metastasis of human hepatocellular carcinoma xenografts are inhibited by small interfering RNA targeting to the subunit ATP6L of proton pump. Cancer Res 2005;65:6843–9.
16. Chessells JM. Recent advances in management of acute leukaemia. Arch Dis Child 2000;82:438–42.
17. Kasamon YL, Swinnen LJ. Treatment advances in adult Burkitt lymphoma and leukemia. Curr Opin Oncol 2004;16:429–35.
18. Nilsson A, De Milito A, Engstrom P, et al. Current chemotherapy protocols for childhood acute lymphoblastic leukemia induce loss of humoral immunity to viral vaccination antigens. Pediatrics 2002;109:e91.
19. Der G. An overview of proton pump inhibitors. Gastroenterol Nurs 2003;26:182–90.
20. Martin de Argila C. Safety of potent gastric acid inhibition. Drugs 2005;65 Suppl 1:97–104.
21. Mattsson JP, Vaananen K, Wallmark B, Lorentzon P. Omeprazole and bafilomycin, two proton pump inhibitors: differentiation of their effects on gastric, kidney and bone H(+)-translocating ATPases. Biochim Biophys Acta 1991;1065:261–8.
22. Moriyama Y, Patel V, Ueda I, Futai M. Evidence for a common binding site for omeprazole and *N*-ethylmaleimide in subunit A of chromaffin granule vacuolar-type H(+)-ATPase. Biochem Biophys Res Commun 1993;196:699–706.
23. Sabolic I, Brown D, Verbavatz JM, Kleinman J. H(+)-ATPases of renal cortical and medullary endosomes are differentially sensitive to Sch-28080 and omeprazole. Am J Physiol 1994;266:F868–77.
24. Luciani F, Spada M, De Milito A, et al. Effect of proton pump inhibitor pretreatment on resistance of solid tumors to cytotoxic drugs. J Natl Cancer Inst 2004;96:1702–13.
25. Martinez-Zaguilan R, Raghunand N, Lynch RM, et al. pH and drug resistance. I. Functional expression of plasmalemmal V-type H^+-ATPase in drug-resistant human breast carcinoma cell lines. Biochem Pharmacol 1999;57:1037–46.
26. Nilsson A, de Milito A, Mowafi F, et al. Expression of CD27-70 on early B cell progenitors in the bone marrow: implication for diagnosis and therapy of childhood ALL. Exp Hematol 2005;33:1500–7.
27. Boya P, Andreau K, Poncet D, et al. Lysosomal membrane permeabilization induces cell death in a mitochondrion-dependent fashion. J Exp Med 2003;197:1323–34.
28. Lin HJ, Herman P, Kang JS, Lakowicz JR. Fluorescence lifetime characterization of novel low-pH probes. Anal Biochem 2001;294:118–25.
29. Nilsson C, Kagedal K, Johansson U, Ollinger K. Analysis of cytosolic and lysosomal pH in apoptotic cells by flow cytometry. Methods Cell Sci 2003;25:185–94.
30. Marches R, Vitetta ES, Uhr JW. A role for intracellular pH in membrane IgM-mediated cell death of human B lymphomas. Proc Natl Acad Sci U S A 2001;98:3434–9.
31. Lugli E, Troiano L, Ferraresi R, et al. Characterization of cells with different mitochondrial membrane potential during apoptosis. Cytometry A 2005;68:28–35.
32. Pui CH, Evans WE. Acute lymphoblastic leukemia. N Engl J Med 1998;339:605–15.
33. Horn J. The proton-pump inhibitors: similarities and differences. Clin Ther 2000;22:266–80; discussion 5.
34. Kroemer G, Jaattela M. Lysosomes and autophagy in cell death control. Nat Rev Cancer 2005;5:886–97.
35. Nakashima S, Hiraku Y, Tada-Oikawa S, et al.

Vacuolar H^+-ATPase inhibitor induces apoptosis via lysosomal dysfunction in the human gastric cancer cell line MKN-1. J Biochem (Tokyo) 2003;134:359–64.
36. Scaringi L, Cornacchione P, Ayroldi E, et al. Omeprazole induces apoptosis in Jurkat cells. Int J Immunopathol Pharmacol 2004;17:331–42.
37. Rich IN, Worthington-White D, Garden OA, Musk P. Apoptosis of leukemic cells accompanies reduction in intracellular pH after targeted inhibition of the Na(+)/H(+) exchanger. Blood 2000;95:1427–34.
38. Nilsson C, Johansson U, Johansson AC, Kagedal K, Ollinger K. Cytosolic acidification and lysosomal alkalinization during TNF-alpha induced apoptosis in U937 cells. Apoptosis 2006;11:1149–59.
39. Dai H, Kramer DL, Yang C, Murti KG, Porter CW, Cleveland JL. The polyamine oxidase inhibitor MDL-72,527 selectively induces apoptosis of transformed hematopoietic cells through lysosomotropic effects. Cancer Res 1999;59:4944–54.
40. Zang Y, Beard RL, Chandraratna RA, Kang JX. Evidence of a lysosomal pathway for apoptosis induced by the synthetic retinoid CD437 in human leukemia HL-60 cells. Cell Death Differ 2001;8:477–85.
41. Bellosillo B, Villamor N, Lopez-Guillermo A, et al. Complement-mediated cell death induced by rituximab in B-cell lymphoproliferative disorders is mediated *in vitro* by a caspase-independent mechanism involving the generation of reactive oxygen species. Blood 2001;98:2771–7.
42. Katashima M, Yamamoto K, Sugiura M, Sawada Y, Iga T. Comparative pharmacokinetic/pharmacodynamic study of proton pump inhibitors, omeprazole and lansoprazole in rats. Drug Metab Dispos 1995;23:718–23.
43. Lugini L, Matarrese P, Tinari A, et al. Cannibalism of live lymphocytes by human metastatic but not primary melanoma cells. Cancer Res 2006;66:3629–38.
44. Izumi H, Torigoe T, Ishiguchi H, et al. Cellular pH regulators: potentially promising molecular targets for cancer chemotherapy. Cancer Treat Rev 2003;29:541–9.
45. De Milito A, Fais S. Proton pump inhibitors may reduce tumour resistance. Expert Opin Pharmacother 2005;6:1049–54.
46. Kountouras J, Boura P, Apostolides G, Zaharioudaki E, Tsapas G. *In vivo* effect of omeprazole on HLA-DR expression and the monocyte-macrophage function in patients with duodenal ulcer disease. Immunopharmacol Immunotoxicol 1994;16:437–48.
47. Sjostrom JE, Kuhler T, Larsson H. Basis for the selective antibacterial activity *in vitro* of proton pump inhibitors against *Helicobacter* spp. Antimicrob Agents Chemother 1997;41:1797–801.
48. Jiang S, Meadows J, Anderson SA, Mukkada AJ. Antileishmanial activity of the antiulcer agent omeprazole. Antimicrob Agents Chemother 2002;46:2569–74.
49. Carlo-Stella C, Di Nicola M, Turco MC, et al. The anti-human leukocyte antigen-DR monoclonal antibody 1D09C3 activates the mitochondrial cell death pathway and exerts a potent antitumor activity in lymphoma-bearing nonobese diabetic/severe combined immunodeficient mice. Cancer Res 2006;66:1799–808.
50. Cregan SP, Dawson VL, Slack RS. Role of AIF in caspase-dependent and caspase-independent cell death. Oncogene 2004;23:2785–96.